



HAL
open science

An unprecedented route of $\bullet\text{OH}$ radical reactivity: ipso-substitution with perhalogenocarbon compounds

Emmanuel Mousset, Nihal Oturan, Mehmet A. Oturan

► To cite this version:

Emmanuel Mousset, Nihal Oturan, Mehmet A. Oturan. An unprecedented route of $\bullet\text{OH}$ radical reactivity: ipso-substitution with perhalogenocarbon compounds. *Applied Catalysis B: Environmental*, 2018, 226, pp.135-156. 10.1016/j.apcatb.2017.12.028 . hal-01712279

HAL Id: hal-01712279

<https://hal.science/hal-01712279>

Submitted on 2 Mar 2018

HAL is a multi-disciplinary open access archive for the deposit and dissemination of scientific research documents, whether they are published or not. The documents may come from teaching and research institutions in France or abroad, or from public or private research centers.

L'archive ouverte pluridisciplinaire **HAL**, est destinée au dépôt et à la diffusion de documents scientifiques de niveau recherche, publiés ou non, émanant des établissements d'enseignement et de recherche français ou étrangers, des laboratoires publics ou privés.

**An unprecedented route of $\cdot\text{OH}$ radical reactivity evidenced by an
electrocatalytical process: ipso-substitution with
perhalogenocarbon compounds**

Emmanuel Mousset^{1,2}, Nihal Oturan¹, Mehmet Oturan^{1,*}

¹ Université Paris-Est, Laboratoire Géomatériaux et Environnement (LGE), EA 4508, UPEM,
5 bd Descartes, 77454 Marne-la-Vallée Cedex 2, France.

² Laboratoire Réactions et Génie des Procédés, UMR CNRS 7274, Université de Lorraine, 1
rue Grandville BP 20451, 54001 Nancy cedex, France.

**Paper submitted to *Applied Catalysis B - Environment*
for consideration**

*Correspondence to:

Mehmet A. Oturan: mehmet.oturan@univ-paris-est.fr

1
2
3
4
5
6
7
8
9
10
11
12
13
14
15
16
17
18
19
20

ABSTRACT

Hydroxyl radical ($\cdot\text{OH}$) is ubiquitous in the environment and in metabolism. It is one of the most powerful oxidants and can react instantaneously with surrounding chemicals. Currently, three attack modes of $\cdot\text{OH}$ have been identified: hydrogen atom abstraction, addition to unsaturated bond and electron transfer. Perhalogenocarbon compounds such as CCl_4 are therefore supposed to be recalcitrant to $\cdot\text{OH}$ as suggested by numerous authors due to the absence of both hydrogen atom(s) and unsaturated bond(s). Here, we report for the first time a fourth attack mode of $\cdot\text{OH}$ through ipso-substitution of the halogen atom. This breakthrough offers new scientific insight for understanding the mechanisms of $\cdot\text{OH}$ oxidation in the related research areas of research. It is especially a great progress in organic contaminants removal from water. In this study, CCl_4 is successfully degraded and mineralized in aqueous media using a green and efficient electrocatalytical production of homogeneous and heterogeneous $\cdot\text{OH}$. Maximum degradation rate of 0.298 min^{-1} and mineralization yield of 82% were reached. This opens up new possibilities of emerging water pollutants elimination such as fluorosurfactants.

Keywords: carbon tetrachloride; anodic oxidation; electrocatalysis; electro-Fenton; oxidation pathway.

21 1. INTRODUCTION

22 The omnipresence of hydroxyl radical ($\cdot\text{OH}$) is now well established in various types of
23 environments including natural waters, atmosphere in which it plays a role of “detergent”,
24 interstellar space as well as biological systems where $\cdot\text{OH}$ has an important role in immunity
25 metabolism [1–4]. It makes $\cdot\text{OH}$ as the most important free radical in chemistry and biology
26 because of its multiple implications and applications [5,6].

27 In water media, $\cdot\text{OH}$ is the second strongest oxidizing agent after fluorine with a standard
28 redox potential of 2.8 V/SHE [7]. The presence of unpaired electron on oxygen atom makes
29 $\cdot\text{OH}$ a very reactive species with a mean lifetime estimated as only a few nanoseconds in
30 water [8]. It destroys most of organic and organometallic pollutants until total mineralization,
31 i.e. conversion into CO_2 , H_2O , and inorganic ions; hence the interest of its use in water
32 treatment area. Indeed, the occurrence of hazardous and toxic pollutants into the water
33 compartments led the water and wastewater regulatory requirements to become more
34 stringent regarding the release of such compounds. Being xenobiotic, these contaminants
35 cannot be removed by conventional wastewater treatment plant and therefore an advanced
36 physicochemical treatment is required. Thus, since more than 30 years the outstanding
37 properties of $\cdot\text{OH}$ have been tested for water purification in the so-called advanced oxidation
38 processes (AOPs) [9]. AOPs have gained increasing interests as they constitute promising,
39 efficient and environmental-friendly methods to remove persistent organic pollutants (POPs)
40 from waters [10,11]. Several types of AOPs have been developed based on the *in situ*
41 formation of $\cdot\text{OH}$ by means of various chemical, photochemical, sonochemical, or
42 electrochemical reactions. Then, the $\cdot\text{OH}$ formed can react according to three possible
43 reaction modes proposed in literature: (i) hydrogen atom abstraction (dehydrogenation), (ii)
44 electrophilic addition to an unsaturated bond (hydroxylation) and (iii) electron transfer
45 (redox) reactions [6,10]. The first mode is typical for alkanes and alcohols (Eq. 1) with rate

46 constants in the range 10^6 - 10^8 $M^{-1} s^{-1}$ [12], whereas the second mode occurs especially with
47 aromatics (ArH) (Eqs. 2a-2b) with rate constants as high as 10^8 - 10^{10} $M^{-1} s^{-1}$ [12] while the
48 third mode is generally given with oxidizable inorganics such as cation (Fe^{2+} (Eq. 3a)) as well
49 as anions (Eq. 3b) (Cl^- , NO_2^- , HCO_3^-) and organics (Eq. 4) [1]:



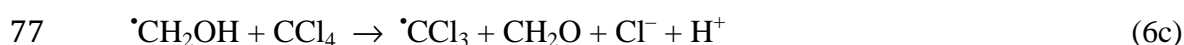
56 Therefore, $\cdot OH$ s are very active species that can oxidize even the most recalcitrant chemicals.
57 However, $\cdot OH$ have been considered in several studies as unreactive with perhalogenated
58 alkanes (C_xX_y) water contaminants that contain only carbon and halogen atoms such as
59 carbon tetrafluoride (CF_4), carbon tetrachloride (CCl_4), hexafluoroethane (C_2F_6) and
60 hexachloroethane (C_2Cl_6) that are widely used as etchant in semiconductor manufacturing and
61 as refrigerants. Indeed, these pollutants do not have any hydrogen atom as well as no
62 unsaturated bond. Thus, no one of the three above-mentioned modes of $\cdot OH$ actions can
63 occur.

64 Interestingly, several authors intended to be able to degrade perhalogenocarbon compounds
65 by applying some AOPs but in the presence of an organic precursor. Cho et al. [13,14]
66 succeeded to degrade CCl_4 with a heterogeneous photocatalysis (UV/ TiO_2) process in the
67 presence of surfactant as organic precursor. It was proposed as a hypothesis that a complex
68 formation between the surfactant functional groups and TiO_2 surface was responsible for the

69 weak visible light absorption and the subsequent photo-induced electron transfer to CCl₄
70 (Eqs. (5a)-(5b)):



73 Gonzalez et al. [15] employed methanol as precursor to mineralize CCl₄ by H₂O₂ photolysis
74 according to the following reactions sequence (Eqs. (6a)-(6c)):



78 In addition, some authors applying other AOPs also demonstrated the degradation of CCl₄ by
79 suggesting the formation of additional inorganic species that were responsible for its
80 decomposition. Thus, it was considered that sonication decomposes water molecules into
81 hydrogen radical ($\cdot\text{H}$) and $\cdot\text{OH}$ and then CCl₄ reacts with $\cdot\text{H}$ [16,17]:



84 In a modified chemical Fenton's treatment it was suggested that the superoxide ion ($\text{O}_2^{\cdot-}$) was
85 responsible for the decomposition of CCl₄ [18–20]. $\text{O}_2^{\cdot-}$ is a weak nucleophile and reductant
86 that was suggested to be able to degrade CCl₄ in aprotic media such as dimethyl sulfoxide and
87 dimethylformamide as organic precursor [21,22] and more recently in aqueous media by
88 using high concentration of H₂O₂ (>0.1 M) in a Fenton-like process.

89 However, an important feature is that at the operated Fenton pH (pH 3 initially), hydroperoxyl
90 ion (HO_2^\bullet), a weak oxidant ($E^\circ = 1.65 \text{ V/SHE}$), predominate in such acidic conditions ($pK_a =$
91 4.8) instead of $\text{O}_2^{\bullet-}$ [23]. Therefore, the role of $\text{O}_2^{\bullet-}$ has to be reconsidered.

92 Recently, electrochemical advanced oxidation processes (EAOPs) for generating $^\bullet\text{OH}$ in a
93 catalytic and continuous mode have gained increasing interests [23–27]. They are not only
94 more environmentally friendly as electron is a clean reagent but also more efficient as they
95 can even degrade the most recalcitrant compounds [28–34] such as cyanuric acid known to be
96 resistant to $^\bullet\text{OH}$ oxidation in more conventional AOPs [35]. Another advantage is that EAOPs
97 are modular process according to the electrodes materials to be used which lead to different
98 oxidizing/reducing species formed [23,36–40]. In other words, the nature of the
99 electrogenerated species can be controlled by the adequate electrode materials and operating
100 conditions. Therefore, the oxidative degradation of perhalogenated compounds such as CCl_4
101 has never been studied by EAOPs, it appears important to carry out it as it can bring novel
102 tremendous scientific insights on the mechanism of degradation of such molecules according
103 to the electrode material employed.

104

105 **2. EXPERIMENTAL**

106 **2.1. Chemicals**

107 All the chemicals were of analytical grade, and were used without any further purification.
108 Carbon tetrachloride (CCl_4), titanium tetrachloride (TiCl_4), potassium hydrogen phthalate,
109 hydrogen peroxide (H_2O_2) (30% w/w) and sodium sulfate (Na_2SO_4) were purchased from
110 Sigma-Aldrich. Heptahydrated ferrous sulfate ($\text{FeSO}_4 \cdot 7\text{H}_2\text{O}$), sulfuric acid (H_2SO_4) and
111 phosphoric acid (H_3PO_4) (85% w/w) were supplied by Acros Organics. In all experiments, the

112 solutions were prepared with ultrapure water from a Millipore Simplicity 185 (resistivity > 18
113 MΩ cm at room temperature).

114

115 **2.2. Electrochemical reactor set-up**

116 Electrolysis experiments with CCl₄ aqueous solutions (0.2 mM) were run at controlled
117 temperature (22.0 ± 0.1 °C), in a 0.20 L closed-undivided glass electrochemical reactor under
118 current-controlled conditions. The cathode was either a 150 cm² carbon felt (CF) piece
119 (Carbone-Lorraine, France) or a 28 cm² plate of stainless steel (SS) (GoodFellow, France).
120 Either a Pt grid (5 cm height cylindrical (i.d. = 3 cm)) or boron-doped diamond (BDD) coated
121 on a Niobium (Nb) plate (28 cm²) (Condias, Germany) was employed as an anode material
122 with an electrode distance of 3.5 cm. The electrochemical cell was monitored by a power
123 supply HAMEG 7042-5 (Germany) and the applied current was set to 1000 mA. An inert
124 supporting electrolyte (Na₂SO₄ at 0.050 M) was added to the medium to ensure a constant
125 ionic strength (0.15 M). The pH of the initial solution was adjusted to a pH of 3 [41]. The
126 solutions were continuously stirred to assure homogeneous mixing. FeSO₄·7H₂O was added
127 (0.05 mM) as a source of catalyst (Fe²⁺) to implement Fenton's reaction in EF process.
128 Compressed air was bubbled initially before starting the experiment and before adding CCl₄
129 compound [42]. This was to saturate the aqueous solution in O₂ as a source of H₂O₂
130 production (Eq. 9) while avoiding the volatilization of CCl₄. The reactor set-up for
131 electrolysis experiments is illustrated in Fig. 1. The same reactor was employed to perform
132 H₂O₂ oxidation experiments, except that the electrodes were absent.

133

134 **2.3. Analytical methods**

135 2.3.1. Cyclic voltammetry (CV)

136 CV experiments were performed to evaluate the electroactivity of CCl_4 in aqueous media with
137 a potentiostat/galvanostat PGP201 VoltaLab (Radiometer Analytical S.A.) in a three-
138 electrode system. Either Pt (1 mm diameter) or glassy carbon (3 mm diameter) was employed
139 as working electrode while a Pt wire was used as counter electrode. A saturated calomel
140 electrode (SCE) was employed as reference electrode; therefore, all the voltage values given
141 in the text are expressed in V/SCE, unless stated otherwise. Sodium sulfate (0.050 M) was
142 used as electrolyte and the solutions were acidified to pH 3.0, the optimal EAOPs conditions.
143 The CV experiments were performed in a voltage range of -3.0 V to +3.0 V and at a scan rate
144 of 10 mV s^{-1} .

145

146 2.3.2. Hydrogen peroxide experiments and analysis

147 The oxidation power of H_2O_2 onto CCl_4 was evaluated by adding initially H_2O_2 in excess
148 (100 mM) into CCl_4 (0.2 mM) aqueous solution before starting the experiments. The amount
149 of H_2O_2 accumulated in bulk solution was determined by performing electrolysis experiments
150 in the same conditions than EAOPs treatments, except that no Fe^{2+} was added to avoid
151 Fenton's reaction to occur [37]. H_2O_2 was quantified by colorimetry using TiCl_4 [43]. The
152 absorbance of the pertitanic acid complex formed was measured with a Perkin Elmer (USA)
153 Lambda 10 UV-VIS spectrophotometer at a wavelength of 410 nm. An external calibration
154 curve was obtained with standards of H_2O_2 , giving a molar extinction coefficient of around
155 $935 \pm 2 \text{ L mol}^{-1} \text{ cm}^{-1}$. The H_2O_2 concentrations were then calculated according to the Beer-
156 Lambert law.

157

158 2.3.3. Total organic carbon (TOC) measurements

159 TOC analyses were performed to quantify the mineralization degree during the different kind
160 of treatments. The solution TOC values were determined by thermal catalytic oxidation (680

161 °C in presence of Pt catalyst) using a Shimadzu (Japan) V_{CSH} TOC analyzer. All samples
162 were acidified to pH 2 with H₃PO₄ (25% w/w) to remove inorganic carbon. The injection
163 volumes were 50 µL. Calibrations were performed by using potassium hydrogen phthalate
164 solutions (50 mg C L⁻¹) as standard. All measured TOC values were given with a coefficient
165 of variance below to 2%.

166 Mineralization yields (r_{min}) were considered equivalent to TOC removal percentage and can
167 be determined according to the following Eq. 8:

$$168 \quad r_{min}(\%) = \frac{(\Delta TOC)_t}{TOC_0} \times 100 \quad (8)$$

169 where $(\Delta TOC)_t$ is the difference between the initial TOC (TOC_0) and TOC at time t.

170

171 2.3.4. Ionic chromatography analysis

172 The inorganic ions released in the treated solutions were determined by ion chromatography
173 using a Dionex ICS-1000 basic ion chromatography system (USA). The analysis of anions
174 was monitored using an IonPac AS4A-SC (25 cm × 4 mm) anion-exchange column linked to
175 an IonPac AG4A-SC (5 cm × 4 mm) column guard. The system was equipped with a DS6
176 conductivity detector containing a cell heated at 35 °C. The mobile phase contained 1.8 mM
177 Na₂CO₃ and 1.7 mM NaHCO₃. The flow rate was set to 2 mL min⁻¹. The suppressor SRS
178 (Self Regenerating Suppressor) needed to prevent the influence of the eluent ions in the
179 detector signal was at a current of 30 mA.

180

181 2.3.5. Kinetic model for CCl₄ degradation

182 The decay rate of CCl₄ can be written as follow (Eq. 9):

$$183 \quad \frac{d[CCl_4]}{dt} = -k_{CCl_4}[\cdot OH][CCl_4] \quad (9)$$

184 where $[CCl_4]$ is the concentration of CCl_4 , k_{CCl_4} is the decay rate constant of CCl_4 and $[\cdot OH]$
 185 is the concentration of $\cdot OH$ radical.

186 Considering that the degradation of one mole of CCl_4 produce four moles of Cl^- , the following
 187 equivalence of chemical rate can be obtained (Eq. 10):

$$188 \quad -\frac{d[CCl_4]}{dt} = +\frac{1}{4} \frac{d[Cl^-]}{dt} \quad (10)$$

189 By inserting Eq. 10 into Eq. 9, the Eq. 11 is given:

$$190 \quad \frac{d[Cl^-]}{dt} = 4k_{CCl_4}[\cdot OH][CCl_4] \quad (11)$$

191 By considering that $[Cl^-] = [CCl_4]_0 - [CCl_4]$, that $[CCl_4] = [CCl_4]_0 - [Cl^-]_{meas}$ and that
 192 $[Cl^-] = 4[Cl^-]_{meas}$, the following Eq. 12 is retrieved from Eq. 11:

$$193 \quad \frac{d[Cl^-]_{meas}}{dt} = k_{CCl_4}[\cdot OH]([CCl_4]_0 - [Cl^-]_{meas}) \quad (12)$$

194 where $[CCl_4]_0$ is the initial concentration of CCl_4 and $[Cl^-]_{meas}$ is the measured concentration
 195 of Cl^- released into the solution.

196 By considering the quasi-steady state approximation towards the $\cdot OH$ concentration evolution,
 197 a pseudo-first order kinetic model can be assumed [23]:

$$198 \quad \frac{d[Cl^-]_{meas}}{dt} = k_{app}([CCl_4]_0 - [Cl^-]_{meas}) \quad (13)$$

199 where $k_{app} = k_{CCl_4}[\cdot OH]$ is the apparent decay rate constant of CCl_4 oxidation by $\cdot OH$.

200 After integration of Eq. 13, the semi-logarithmic Eq. 14 is obtained:

$$201 \quad \ln\left(\frac{[CCl_4]_0}{[CCl_4]_0 - [Cl^-]_{meas}}\right) = \ln\left(\frac{[CCl_4]_0}{[CCl_4]_t}\right) = k_{app}t \quad (14)$$

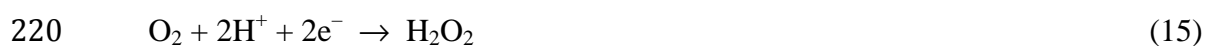
202 where $[CCl_4]_t$ is the concentration of CCl_4 at time t .

203

204 3. RESULTS AND DISCUSSION

205 3.1. Evaluation of electroactivity of CCl₄

206 Before studying the possibility of CCl₄ degradation by $\cdot\text{OH}$ produced by EAOPs, it appeared
207 important to preliminary verify the electroactivity of CCl₄ to check if it can be degraded by
208 direct electron transfer at anode or cathode surface. Cyclic voltammetry (CV) have been
209 therefore performed in voltage window ranging from -3 V to +3 V in Na₂SO₄ (0.050 M)
210 solution at pH 3. Either platinum (Pt) or glassy carbon was used as working electrode, since
211 both electrode materials were later employed in the EAOPs. As anticipated, neither electro-
212 oxidation nor electro-reduction of CCl₄ occurred by using Pt as working electrode (Fig. 2A).
213 Whatever the presence or not of CCl₄, no peak of current was observed except the oxidation
214 of H₂O into O₂ (anode) and its reduction into H₂ (cathode). Employing vitreous carbon as
215 working electrode further demonstrated the non-electroactivity of CCl₄ at the potential range
216 studied (Fig. 2B). A difference was noticed between Pt and carbon electrode, since a cathodic
217 peak, attributed to the formation of H₂O₂ (Eq. 15), was noticed at -0.6 V with the latter. This
218 peak is expected because carbonaceous cathodes are well-known to promote the formation of
219 H₂O₂ from 2-electron reduction of O₂ [44]:



221 To further investigate the oxidative inaction of H₂O₂ towards CCl₄, experiments were
222 performed by initially spiking H₂O₂ in excess (100 mM) in a 0.2 mM CCl₄ aqueous solution
223 in a hermetic seal batch reactor (Fig. 2C and Fig. 1). As expected H₂O₂ was not able to
224 degrade CCl₄ as no Cl⁻ were released in solution while the total organic carbon (TOC) values
225 remained unchanged along the experiment. The H₂O₂ concentration measurements depicted in
226 Fig. 3 highlights the absence of H₂O₂ consumption during oxidation experiments with CCl₄,
227 as it remained constant (around 100 ± 0.1 mM) all along the experiment. H₂O₂ is known to be

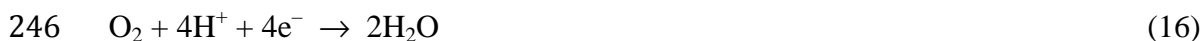
228 a relatively weak oxidant ($E^\circ(\text{H}_2\text{O}_2/\text{H}_2\text{O}) = 1.8 \text{ V/SHE}$) [45] that has relatively poor redox
229 abilities which explain its unreliability to oxidize CCl_4 .

230

231 **3.2. Degradation of CCl_4 by EAOPs**

232 3.2.1. Role of BDD anode: production of heterogeneous $\cdot\text{OH}$

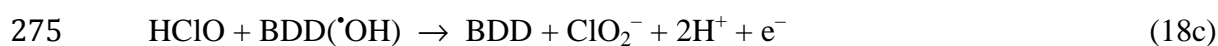
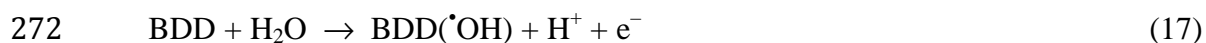
233 The performance of EAOPs to degrade CCl_4 (0.2 mM) has been tested. Guided by the
234 hypothesis described in section 3.1 regarding the role of $\cdot\text{OH}$ in the CCl_4 degradation, an
235 anodic oxidation (AO) experiment was first performed with a SS cathode and a BDD anode
236 (AO-SS/BDD cell) in order to check this assumption (Fig. 4A). The experiments were
237 performed in aqueous media, in absence of any other organic compound that could play a role
238 of precursor for $\cdot\text{CCl}_3$ formation. Moreover, the electrolysis was carried out in dark conditions
239 to avoid any photo-activity. To check whether H_2O_2 formation occurred at SS cathode, the
240 accumulation of H_2O_2 in bulk solution during electrolysis using SS cathode and Pt anode has
241 been performed and the results are represented in Fig. 5. It is shown that the H_2O_2
242 concentration could not reach higher value than 0.041 mM, which is very low. This is
243 attributed to the SS material that do not favor the two electrons-oxygen reduction reaction
244 (ORR) pathway to form H_2O_2 and will rather promote the four electron-ORR pathway that
245 produce H_2O (Eq. 16) as previously stated [23,43]:

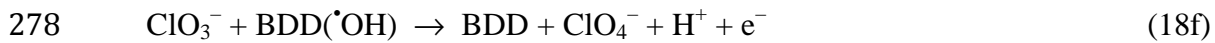
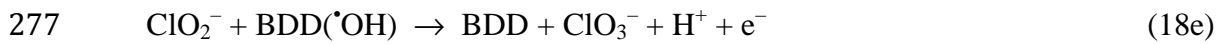


247 Therefore, the use of SS cathode limited the formation of H_2O_2 through O_2 reduction (Eq. 15)
248 (Fig. 5) while the BDD anode ensured the heterogeneous generation of BDD($\cdot\text{OH}$) thanks to
249 its high O_2 evolution overvoltage (2.3 V/SHE) [46,47].

250 Excitingly, Fig. 4A highlights the release of Cl^- ions into the solution by performing an AO-
251 SS/BDD experiment. Upon control experiments results showing, as expected, the absence of

252 Cl^- ions in solution when no current intensity was applied, CCl_4 was successfully degraded by
 253 $\text{BDD}(\cdot\text{OH})$ generated in AO process. It can further be noticed that the amount of Cl^- formed
 254 could not reach the maximal Cl^- theoretical concentration ($[\text{Cl}^-]_{\text{max,th}}$) that could be released.
 255 In fact, the rate of chloride formation was in competition with the rate of its oxidation into Cl_2
 256 as highlighted by the decrease of $[\text{Cl}^-]$ after 40 min of treatment (Fig. 4A). Indeed, Cl_2 react
 257 quickly with H_2O to form HOCl [48] that undergoes further oxidation reactions to be
 258 converted into chlorate (ClO_3^-) and perchlorate (ClO_4^-) at BDD surface as shown by ionic
 259 chromatograms in Fig. 6. Thus, the chromatograms of anions evolution during EF treatment
 260 with BDD anode at different treatment time (0 min, 20 min, 40 min, 60 min, 120 min, and
 261 240 min) display Cl^- peaks at retention time around 1.3 min and major peaks of SO_4^{2-} at
 262 retention time of 3.1 min. Interestingly, two more peaks could be distinguished at retention
 263 times of 2.2 min and 7.4 min, respectively. These peaks are ascribed to chlorine oxyanions
 264 such as ClO_3^- and ClO_4^- , respectively. These anions can be formed by Cl^- oxidation into Cl_2
 265 gas at BDD anode due to its high oxidation ability with physisorbed $\cdot\text{OH}$ formed at its surface
 266 ($\text{BDD}(\cdot\text{OH})$) (Eqs. 17-18a). Cl_2 reacts quickly with H_2O to form the hypochlorous acid
 267 (HClO) (Eq. 8b) in the bulk. Since the pH remained between 2.4 and 3.0 during the whole
 268 electrolysis, HClO is the predominant species as compared to ClO^- knowing the acid
 269 dissociation constant value of HClO ; $pK_a = 7.54$ (at 25 °C). HClO is then oxidized into ClO_2^-
 270 (Eq. 18c) which is quickly oxidized into ClO_3^- (Eqs. 18d-18e) and then into ClO_4^- (Eq. 18f)
 271 as end-product having the maximal oxidation state [49,50]:





279 Chlorite ion was not observed in the electrolysis with BDD because the high applied current
 280 density (35.7 mA cm^{-2} as reported to the BDD anode surface area) favor the rapid oxidation
 281 of ClO_2^- into ClO_3^- as noticed previously [51], especially in BDD experiments performed at
 282 30 mA cm^{-2} [52].

283 As it can be seen at the detailed view of Cl^- peak evolution (Fig. 6B), a maximal peak area
 284 could be noticed at 20 min of electrolysis, while it started decreasing after longer treatment.
 285 At this time the peaks area of ClO_3^- increase until 60 min of treatment and start decreasing
 286 after electrolysis time longer than 120 min. In the meanwhile, peaks area of ClO_4^- start raising
 287 from 120 min until 240 min of treatment. The subsequent increase/decrease trends observed
 288 from Cl^- evolution concentration to ClO_3^- and then to ClO_4^- corroborated the reactions
 289 sequence (Eqs. 18a-18e).

290 In addition, the chromatogram of SO_4^{2-} (Fig. 6C) highlights a slight decrease of SO_4^{2-} peak
 291 right after the starting of the EF-CF/BDD treatment, corresponding to a SO_4^{2-} concentration
 292 decrease from 50 mM to $47.1 \pm 0.9 \text{ mM}$. This is attributed to the reaction of SO_4^{2-} with high
 293 reactive BDD surface producing sulfate radical (SO_4^\cdot) (Eq. 19a) and persulfate ($\text{S}_2\text{O}_8^{2-}$) (Eq.
 294 19b) as previously stated [53,54].



297 The oxidation power of SO_4^\cdot and $\text{S}_2\text{O}_8^{2-}$ are lower than that of the $\cdot\text{OH}$, with standard
 298 reduction potentials of 2.6 and 2.01 V/SHE, respectively [23]. It has been previously
 299 demonstrated that SO_4^\cdot radical could not react with CCl_4 , since it was found as one of the end-

300 product during oxidation of chlorinated phenol by SO_4^\bullet radical [55]. It means that $\bullet\text{OH}$ is the
301 only species responsible for the oxidation of CCl_4 .

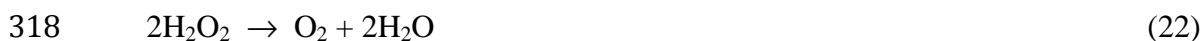
302 It is important to note that the same trends were observed with all BDD experiments (AO-
303 SS/BDD, AO-CF/BDD and EF-CF/BDD) as these phenomenon depends on the use of BDD
304 anode material itself.

305

306 3.2.2. Influence of CF cathode: production of homogeneous $\bullet\text{OH}$ by peroxone reaction

307 Interestingly, when a CF cathode was employed (AO-CF/BDD cell), the concentration of Cl^-
308 released could reach $[\text{Cl}^-]_{\text{max,th}}$ (0.8 mM), highlighting a better degradation of CCl_4 (Fig. 4A).

309 To better understand this behavior, the accumulation of H_2O_2 in bulk solution during
310 electrolysis using CF cathode and Pt anode is represented in Fig. 7. It was first noticed a
311 transient phase followed by a steady state. This phenomenon is typical in undivided cell study
312 and is referred to the competition reactions between H_2O_2 electrogeneration and H_2O_2
313 decomposition at the anode (Eqs. 20a-20b), at the cathode (Eq. 21) and in a lesser extent
314 decomposition in bulk solution (Eq. 22) as stated previously by numerous authors [23]:



319 It was further emphasized that in presence of CF cathode the maximal amount of H_2O_2
320 accumulated in bulk solution was 1 mM, which was 24 times higher than with SS cathode. It
321 was attributed to the nature of cathode material itself and to its surface area. Indeed, carbon-
322 based cathodes have high H_2 evolution overpotential and low catalytic activity for H_2O_2
323 decomposition. Moreover, CF has a 3D porous structure that dramatically increases its

324 specific surface area as compared to the SS material employed. This property makes increase
325 the number of active sites for O₂ adsorption before its subsequent reduction into H₂O₂.
326 Therefore, the enhancement obtained with AO-CF/BDD cell as compared to AO-SS/BDD cell
327 could be due to the additional source of $\cdot\text{OH}$ formed by peroxone reaction between H₂O₂
328 electrogenerated at CF cathode and O₃ produced at the anode surface (Eq. 23) [56], as
329 previously shown in several studies performed in similar electrolysis conditions [57–59], thus
330 confirming the role of $\cdot\text{OH}$ in the degradation process.



332 Indeed the high oxidation power of BDD anode allows also generating O₃ from water
333 oxidation at its surface (Eq. 24) [49].



335 It is worthy to specify that O₃ itself is a moderately strong oxidant ($E^\circ(\text{O}_3/\text{O}_2) = 2.1 \text{ V/SHE}$)
336 [45] compared to $\cdot\text{OH}$ and has no direct oxidation effect on CCl₄ as stated by a previous study
337 [19].

338

339 3.2.3. Role of iron catalyst: production of homogeneous $\cdot\text{OH}$ by Fenton reaction

340 The addition of Fe²⁺ (0.1 mM) in order to produce $\cdot\text{OH}$ through Fenton's reaction (Eq. 25)
341 [23] was further investigated by performing electro-Fenton (EF) treatment with CF cathode
342 and BDD anode (EF-CF/BDD cell).



344 The presence of ferrous ion could even enhance better the degradation of CCl₄ by reaching
345 faster $[\text{Cl}^-]_{\text{max,th}}$ value as seen in Fig. 4A.

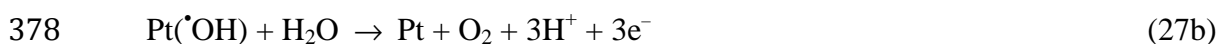
346 This enhancement in CCl₄ degradation rate is due to the formation of homogeneous [•]OH
347 formed in bulk solution that react directly with CCl₄, in addition to BDD([•]OH) formed at
348 anode surface. In this process, Fenton's reaction (Eq. 25) is electrocatalyzed by continuous
349 regeneration of Fe²⁺ (catalyst) from electro-reduction of Fe³⁺ ions (Eq. 26) formed by Fenton's
350 reaction [48]:



352 The difference of efficiency between AO-CF/BDD and EF-CF/BDD experiments was
353 therefore mainly attributed to the action of supplementary [•]OH generated in the bulk solution
354 by Fenton reaction (Eq. 25).

355 Furthermore, when Pt was used as anode instead of BDD in EF process (EF-CF/Pt cell), the
356 dechlorination rate and yield were higher compared with AO-SS/BDD cell (Fig. 4A). It was
357 also noticed that a plateau of Cl⁻ concentration was observed in EF-CF/Pt cell experiment,
358 highlighting the accumulation of Cl⁻ in the solution. In order to better understand this
359 evolution, the chromatograms of anions evolution during EF treatment with Pt anode at
360 different treatment time (0 min, 5 min, 10 min, 20 min, 40 min, 60 min, 120 min, 180 min,
361 240 min) have been recorded and are represented in Fig. 8. Fig. 8A displays Cl⁻ peaks at
362 retention time around 1.3 min and major peaks of SO₄²⁻ from the supporting electrolyte
363 (Na₂SO₄) at retention time of 3.1 min, as observed with BDD anode electrolysis. To have a
364 better view of the Cl⁻ chromatograms, an enlarged picture allows observing the evolution of
365 Cl⁻ peaks area and height in Fig. 8B. From 0 min to 40 min of EF treatment, it is clearly seen
366 an increase of peak area, meaning that CCl₄ is progressively degraded into Cl⁻. After 40 min
367 of treatment the peaks area barely change, because at this time, the concentration of Cl⁻ has
368 reached its theoretical level value (0.8 mM). Moreover, no other peak could be observed on
369 the chromatogram whatever the time of treatment, meaning that chloride ions could not be

370 further oxidized into Cl₂, chlorate, perchlorate species on the contrary to BDD experiments. It
371 is also interesting to note that the peaks area of SO₄²⁻ remain the same (50 ± 0.1 mM)
372 whatever the treatment time (Fig. 8C), which underlines that the electrolyte stayed unreactive
373 during the treatment, unlike with BDD treatments. This is in accordance with the low
374 oxidation power of Pt that has a low O₂ evolution overvoltage (1.6 V/SHE) [60]. In this case,
375 •OH at Pt surface (Pt(•OH)) is chemisorbed and O₂ evolution is the main reaction (Eqs. 27a-
376 27b) [47]:



379 In addition, [Cl⁻]_{max,th} (0.8 mM) was reached only after 120 min against around 20 min with
380 AO-CF/BDD and EF-CF/BDD cells. The superiority of AO-CF/BDD cell over EF-CF/Pt cell
381 was attributed to the higher oxidation power of BDD and to the second source of •OH from
382 peroxone reaction as discussed in section 3.2.2.

383 Thus, the only source of •OH was coming from the electro-Fenton process through Fenton's
384 reaction in EF-CF/Pt cell. It further emphasized the primary role of homogeneous •OH formed
385 by Fenton's reaction as compared to heterogeneous •OH formed at BDD surface in AO-
386 SS/BDD cell, because in such diluted solution the electrolysis is controlled by mass transfer
387 rate.

388

389 3.2.4. Quantitative comparison between oxidation mechanisms with kinetic rate 390 constants

391 In order to compare quantitatively each applied condition, a kinetic model has been
392 established (section 2.3.5). The kinetic rate constants of CCl₄ degradation (*k_{app}*) have been

393 determined considering a pseudo-first order kinetics for the reaction between CCl_4 and $\cdot\text{OH}$
394 by assuming a quasi-stationary state for $\cdot\text{OH}$ concentration.

395 Based on Eq. 14, a linear regression allowed determining k_{app} values from the slope of the
396 straight lines (Fig. 4B) that were ranked as follow: AO-SS/BDD ($0.004 \pm 0.001 \text{ min}^{-1}$) < EF-
397 CF/Pt ($0.072 \pm 0.003 \text{ min}^{-1}$) < AO-CF/BDD ($0.171 \pm 0.002 \text{ min}^{-1}$) < EF-CF/BDD ($0.298 \pm$
398 0.001 min^{-1}). All correlation coefficient (R^2) were higher than 0.989, highlighting the good
399 fitting between experimental data and the pseudo-first order kinetic model. This rank was
400 corroborating the dechlorination results. It highlights again the primary role of BDD($\cdot\text{OH}$) /
401 $\cdot\text{OH}$ while EF-CF/BDD depicted more than 4 times quicker degradation kinetics due to the
402 three sources of hydroxyl radicals generation (e.g. Fenton, peroxone and anodic oxidation
403 mechanisms co-contributions).

404

405 **3.3. Mineralization of CCl_4 by EAOPs**

406 The mineralization of CCl_4 was evaluated by monitoring the TOC in the same experimental
407 conditions, e.g. AO-SS/BDD, AO-CF/BDD, EF-CF/BDD and EF-CF/Pt cells (Fig. 9). After 8
408 h of electrolysis, the following mineralization rank was obtained: AO-SS/BDD ($24 \pm 1.2 \%$) <
409 EF-CF/Pt ($55 \pm 1.8 \%$) < AO-CF/BDD ($74 \pm 0.9 \%$) < EF-CF/BDD ($82 \pm 1.4 \%$) (Fig. 9A). In
410 addition, by assuming a pseudo-first order kinetic model for TOC decay [61], the same rank
411 was noticed: AO-SS/BDD ($0.123 \pm 0.011 \text{ h}^{-1}$) < EF-CF/Pt ($0.220 \pm 0.013 \text{ h}^{-1}$) < AO-CF/BDD
412 ($0.772 \pm 0.012 \text{ h}^{-1}$) < EF-CF/BDD ($0.806 \pm 0.010 \text{ h}^{-1}$) (Fig. 9B). All correlation coefficient
413 (R^2) values were higher than 0.989, highlighting again the good fitting between experimental
414 data and the pseudo-first order kinetic model.

415 Knowing that the control experiment has shown negligible TOC removal (2% in 8 h-
416 electrolysis), we could first conclude that CCl_4 was successfully mineralized even with AO-

417 SS/BDD giving the lower production of $\cdot\text{OH}$ as mentioned previously. Moreover, these ranks
418 of mineralization efficiency were corroborating the degradation kinetics results,
419 demonstrating again the superiority of EF-CF/BDD.

420

421 3.4. Proposed reaction pathway

422 Based on the above finding a reaction pathway for $\cdot\text{OH}$ action on CCl_4 is proposed (Fig.
423 10A). For the sake of simplicity, hydroxyl radicals were presented by $\cdot\text{OH}$ without making
424 explicit the O-H bond. First, the presence of Cl atom favors the formation of a dipole between
425 C(δ^+) and Cl(δ^-), atoms due to the higher electronegativity of Cl (3.16) compared to C (2.55)
426 according to Pauling scale. Being a strong electrophilic species, $\cdot\text{OH}$ reacts by ipso-
427 substitution on the C atom (Eq. 28a) leading to the subsequent formation of trichloromethanol
428 (CCl_3OH) (Eq. 28b). Trichloromethanol is then decomposed in water into phosgene (CCl_2O)
429 (Eq. 29) [62]. Finally CCl_2O is quickly hydrolyzed in water by forming CO_2 , Cl^- and H^+ (Eq.
430 30) [63].



435 Taking into account these considerations, a reaction pathway was therefore proposed for
436 complete degradation of CCl_4 until mineralization, leading to a new attack mode of $\cdot\text{OH}$ (Fig.
437 10B). Over the existing attack $\cdot\text{OH}$ modes, e.g. dehydrogenation, hydroxylation and electron
438 transfer [6,64], a fourth mode, namely “**ipso-substitution**” is proposed. It generally consists
439 of the oxidation of perhalogenocarbon compounds (C_xX_y) into trihalo-alcohol ($\text{C}_x\text{X}_{y-1}\text{OH}$) in

440 a first step. Furthermore, it has been observed a slight continuous decrease of pH during the
441 EAOPs treatments from an initial pH of 3.0 to a final pH of around 2.4 ± 0.2 after 8 h
442 electrolysis with a standard deviation of 0.2 which is due to the kind of applied treatment.
443 This is an evidence of the accumulation of protons formed through the mechanism proposed.

444

445 **4. CONCLUSIONS**

446 In summary, the treatment of CCl_4 in aqueous solution with EAOPs has been investigated for
447 the first time. Upon successful degradation and mineralization of CCl_4 with the unique
448 presence of $\cdot\text{OH}$ produced by anodic oxidation a new attack mode of $\cdot\text{OH}$ was proposed on
449 perhalogenocarbon compounds by ipso-substitution of halogen atom with $\cdot\text{OH}$. The decrease
450 of pH during the electrolysis corroborated the proposed mechanism. The use of electro-
451 Fenton process enhanced significantly the removal efficiency due to generation of
452 supplementary $\cdot\text{OH}$ in the bulk solution.

453 This fourth oxidation pathway of $\cdot\text{OH}$ should be considered in other areas of research such as
454 in atmospheric studies as some of these perhalogenocarbons are known to be volatile and can
455 be subjected to $\cdot\text{OH}$ reactions.

456 Furthermore, this new finding opens up many opportunities in environmental protection by
457 offering possibilities of degrading and mineralizing such recalcitrant perhalogenocarbons
458 compounds that are used as solvents, refrigerant, aerosol propellant and representing an
459 environmental issue, such as carbon tetrafluoride, hexafluoroethane, carbon tetrachloride,
460 hexachloroethane, perfluorohexane, and so on, but also cyclic perfluoroalkanes like
461 perfluorooctane, perfluoro-1,3-dimethylcyclohexane and perfluorodecalin. More recently
462 fluorosurfactants such as perfluorooctanesulfonic acid, perfluorononanoic acid and
463 perfluorooctanoic acid have been found into the environment and especially into water

464 bodies. They are employed by some textile companies in emulsion polymerization process to
465 produce fluoropolymers but they have caught recently the attention of regulatory agencies has
466 they are persistent in the environment, toxic and bioaccumulate in the food chain.

467 In short, this study highlights that perhalogenocarbons compounds should be considered to be
468 eliminated by $\cdot\text{OH}$ generated in EAOPs.

469

470 **REFERENCES**

- 471 [1] S. Gligorovski, R. Streckowski, S. Barbati, D. Vione, Environmental Implications of
472 Hydroxyl Radicals ($\cdot\text{OH}$), *Chem. Rev.* 115 (2015) 13051–13092.
- 473 [2] S. Li, J. Matthews, A. Sinha, Atmospheric Hydroxyl Radical Production from
474 Electronically Excited NO_2 and H_2O , *Science* 319 (2008) 1657–1660.
- 475 [3] W.H. Rodebush, C.R. Keizer, F.S. McKee, J. V. Quagliano, The Reactions of the
476 Hydroxyl Radical, *J. Am. Chem. Soc.* 69 (1947) 538–540.
- 477 [4] J. Vieceli, L.X. Dang, B.C. Garrett, D.J. Tobias, B. Finlayson-pitts, S. Hunt, P.
478 Jungwirth, Hydroxyl Radical at the Air - Water Interface, *J. Am. Chem. Soc.* 126
479 (2004) 16308–16309.
- 480 [5] P.A. Riley, Free radicals in biology: oxidative stress and the effects of ionizing
481 radiation., *Int. J. Radiat. Biol.* 65 (1994) 27–33.
- 482 [6] L.M. Dorfman, G.E. Adams, Reactivity of the hydroxyl radical in aqueous solutions,
483 (1973) 59 pp.
- 484 [7] W.M. Latimer, Oxidation potentials, *Soil Sci.* 74 (1952) 333.
- 485 [8] E.G. Janzen, Y. Kotake, R.D. Hinton, Stabilities of hydroxyl radical spin of PBN-type
486 spin traps, *Free Radic. Biol. Med.* 12 (1992) 169–173.
- 487 [9] W.H. Glaze, J.W. Kang, D.H. Chapin, The chemistry of water-treatment processes
488 involving ozone, hydrogen-peroxide and ultraviolet-radiation, *Ozone Sci. Eng.* 9
489 (1987) 335–352.
- 490 [10] M.A. Oturan, J.-J. Aaron, Advanced Oxidation Processes in Water/Wastewater
491 Treatment: Principles and Applications. A Review, *Crit. Rev. Environ. Sci. Technol.*
492 44 (2014) 2577–2641.
- 493 [11] M. Pelaez, N.T. Nolan, S.C. Pillai, M.K. Seery, P. Falaras, A.G. Kontos, P.S.M.

- 494 Dunlop, J.W.J. Hamilton, J.A. Byrne, K. O'Shea, M.H. Entezari, D.D. Dionysiou, A
495 review on the visible light active titanium dioxide photocatalysts for environmental
496 applications, *Appl. Catal. B Environ.* 125 (2012) 331–349.
- 497 [12] G.V Buxton, C.L. Greenstock, W.P. Helman, A.B. Ross, Critical Review of Rate
498 Constants for Reactions of Hydrated Electrons, Hydrogen Atoms and Hydroxyl
499 Radicals ($\cdot\text{OH}/\cdot\text{O}^-$) in Aqueous Solution, *J. Phys. Chem. Ref. Data.* 17 (1988) 513–886.
- 500 [13] Y. Cho, H. Kyung, W. Choi, Visible light activity of TiO_2 for the photoreduction of
501 CCl_4 and Cr(VI) in the presence of nonionic surfactant (Brij), *Appl. Catal. B Environ.*
502 52 (2004) 23–32.
- 503 [14] Y. Cho, H. Park, W. Choi, Novel complexation between ferric ions and nonionic
504 surfactants (Brij) and its visible light activity for CCl_4 degradation in aqueous micellar
505 solutions, *J. Photochem. Photobiol. A Chem.* 165 (2004) 43–50.
- 506 [15] M.C. Gonzalez, G.C. Le Roux, J.A. Rosso, A.M. Braun, Mineralization of CCl_4 by the
507 UVC-photolysis of hydrogen peroxide in the presence of methanol., *Chemosphere.* 69
508 (2007) 1238–44.
- 509 [16] M. Lee, J. Oh, Sonolysis of trichloroethylene and carbon tetrachloride in aqueous
510 solution., *Ultrason. Sonochem.* 17 (2010) 207–212.
- 511 [17] M. Lim, Y. Son, J. Khim, Frequency effects on the sonochemical degradation of
512 chlorinated compounds., *Ultrason. Sonochem.* 18 (2011) 460–465.
- 513 [18] H. Che, W. Lee, Selective redox degradation of chlorinated aliphatic compounds by
514 Fenton reaction in pyrite suspension., *Chemosphere.* 82 (2011) 1103–1108.
- 515 [19] A.L. Teel, R.J. Watts, Degradation of carbon tetrachloride by modified Fenton's
516 reagent, *J. Hazard. Mater.* 94 (2002) 179–189.
- 517 [20] B.A. Smith, A.L. Teel, R.J. Watts, Mechanism for the destruction of carbon
518 tetrachloride and chloroform DNAPLs by modified Fenton's reagent., *J. Contam.*

- 519 Hydrol. 85 (2006) 229–46.
- 520 [21] J.L. Roberts, D.T. Sawyer, Facile degradation by superoxide ion of carbon
521 tetrachloride, chloroform, methylene chloride, and p,p'-DDT in aprotic media, J. Am.
522 Chem. Soc. 103 (1981) 712.
- 523 [22] J.L. Roberts, T.S. Calderwood, D.T. Sawyer, Oxygenation by Superoxide Ion of CCl₄,
524 FCl₃, HCCl₃, p,p'-DDT, and Related Trichloromethyl Substrates (RCCl₃) in Aprotic
525 Solvents, J. Am. Chem. Soc. 105 (1983) 7691–7696.
- 526 [23] E. Brillas, I. Sirés, M.A. Oturan, Electro-Fenton Process and Related Electrochemical
527 Technologies Based on Fenton's Reaction Chemistry, Chem. Rev. 109 (2009) 6570–
528 6631.
- 529 [24] M.A. Rodrigo, N. Oturan, M.A. Oturan, Electrochemically assisted remediation of
530 pesticides in soils and water: a review, Chem. Rev. 114 (2014) 8720–8745.
- 531 [25] C.A. Martinez-Huitle, M.A. Rodrigo, I. Sires, O. Scialdone, Single and Coupled
532 Electrochemical Processes and Reactors for the Abatement of Organic Water
533 Pollutants : A Critical Review, Chem. Rev. 115 (2015) 13362–13407.
- 534 [26] I. Sirés, E. Brillas, M.A. Oturan, M.A. Rodrigo, M. Panizza, Electrochemical advanced
535 oxidation processes: today and tomorrow. A review., Environ. Sci. Pollut. Res. Int. 21
536 (2014) 8336–8367.
- 537 [27] F.C. Moreira, R.A.R. Boaventura, E. Brillas, V.J.P. Vilar, Electrochemical advanced
538 oxidation processes: A review on their application to synthetic and real wastewaters,
539 Appl. Catal. B Environ. 202 (2017) 217–261.
- 540 [28] E. Mousset, L. Frunzo, G. Esposito, E.D. van Hullebusch, N. Oturan, M.A. Oturan, A
541 complete phenol oxidation pathway obtained during electro-Fenton treatment and
542 validated by a kinetic model study, Appl. Catal. B Environ. 180 (2016) 189–198.
- 543 [29] F.C. Moreira, R.A.R. Boaventura, E. Brillas, V.J.P. Vilar, Degradation of trimethoprim

- 544 antibiotic by UVA photoelectro-Fenton process mediated by Fe(III)-carboxylate
545 complexes, *Appl. Catal. B Environ.* 162 (2015) 34–44.
- 546 [30] F. Yu, M. Zhou, X. Yu, Cost-effective electro-Fenton using modified graphite felt that
547 dramatically enhanced on H₂O₂ electro-generation without external aeration,
548 *Electrochim. Acta.* 163 (2015) 182–189.
- 549 [31] E. Mousset, D. Huguenot, E.D. Van Hullebusch, N. Oturan, G. Guibaud, G. Esposito,
550 M.A. Oturan, Impact of electrochemical treatment of soil washing solution on PAH
551 degradation efficiency and soil respirometry, *Environ. Pollut.* 211 (2016) 354–362.
- 552 [32] D.M. De Araújo, C. Sáez, C.A. Martínez-Huitle, P. Cañizares, M.A. Rodrigo, Influence
553 of mediated processes on the removal of Rhodamine with conductive-diamond
554 electrochemical oxidation, *Appl. Catal. B Environ.* 166–167 (2015) 454–459.
- 555 [33] F.C. Moreira, R.A.R. Boaventura, E. Brillas, V.J.P. Vilar, Degradation of trimethoprim
556 antibiotic by UVA photoelectro-Fenton process mediated by Fe(III)-carboxylate
557 complexes, *Appl. Catal. B Environ.* 162 (2015) 34–44.
- 558 [34] E. Mousset, N. Oturan, E.D. van Hullebusch, G. Guibaud, G. Esposito, M.A. Oturan,
559 Influence of solubilizing agents (cyclodextrin or surfactant) on phenanthrene
560 degradation by electro-Fenton process - Study of soil washing recycling possibilities
561 and environmental impact, *Water Res.* 48 (2014) 306-316.
- 562 [35] N. Oturan, E. Brillas, M.A. Oturan, Unprecedented total mineralization of atrazine and
563 cyanuric acid by anodic oxidation and electro-Fenton with a boron-doped diamond
564 anode, *Environ. Chem. Lett.* 10 (2012) 165–170.
- 565 [36] E. Mousset, N. Oturan, E.D. van Hullebusch, G. Guibaud, G. Esposito, M.A. Oturan,
566 Treatment of synthetic soil washing solutions containing phenanthrene and
567 cyclodextrin by electro-oxidation. Influence of anode materials on toxicity removal and
568 biodegradability enhancement, *Appl. Catal. B Environ.* 160–161 (2014) 666–675.

- 569 [37] E. Mousset, Z. Wang, J. Hammaker, O. Lefebvre, Physico-chemical properties of
570 pristine graphene and its performance as electrode material for electro-Fenton
571 treatment of wastewater, *Electrochim. Acta.* (2016).
- 572 [38] E. Mousset, Z.T. Ko, M. Syafiq, Z. Wang, O. Lefebvre, Electrocatalytic activity
573 enhancement of a graphene ink-coated carbon cloth cathode for oxidative treatment,
574 *Electrochim. Acta.* 222 (2016) 1628–1641.
- 575 [39] P.V. Nidheesh, R. Gandhimathi, Trends in electro-Fenton process for water and
576 wastewater treatment: An overview, *Desalination.* 299 (2012) 1–15.
- 577 [40] T.X.H. Le, M. Bechelany, S. Lacour, N. Oturan, M. a. Oturan, M. Cretin, High
578 removal efficiency of dye pollutants by electron-Fenton process using a graphene
579 based cathode, *Carbon N. Y.* 94 (2015) 1003–1011.
- 580 [41] E. Mousset, N. Oturan, E.D. van Hullebusch, G. Guibaud, G. Esposito, M.A. Oturan, A
581 new micelle-based method to quantify the Tween 80[®] surfactant for soil remediation,
582 *Agron. Sustain. Dev.* 33 (2013) 839–846.
- 583 [42] E. Mousset, Z. Wang, O. Lefebvre, Electro-Fenton for control and removal of
584 micropollutants - process optimization and energy efficiency, *Water Sci. Technol.* 74
585 (2016) 2068-2074.
- 586 [43] F. Sopaj, Study of the influence of electrode material in the application of
587 electrochemical advanced oxidation processes to removal of pharmaceutical pollutants
588 from water, PhD thesis, University of Paris-Est, 2013.
- 589 [44] N. Oturan, J. Wu, H. Zhang, V.K. Sharma, M.A. Oturan, Electrocatalytic destruction of
590 the antibiotic tetracycline in aqueous medium by electrochemical advanced oxidation
591 processes: Effect of electrode materials, *Appl. Catal. B Environ.* 140–141 (2013) 92–
592 97.
- 593 [45] A.J. Bard, R. Parsons, J. Jordan, *Standard Potentials in Aqueous Solutions*, 1985.

- 594 [46] B. Marselli, J. Garcia-Gomez, P.-A. Michaud, M.A. Rodrigo, C. Comninellis,
595 Electrogeneration of Hydroxyl Radicals on Boron-Doped Diamond Electrodes, J.
596 Electrochem. Soc. 150 (2003) D79–D83.
- 597 [47] M. Panizza, G. Cerisola, Direct and mediated anodic oxidation of organic pollutants.,
598 Chem. Rev. 109 (2009) 6541–6569.
- 599 [48] I. Sirés, J.A. Garrido, R.M. Rodríguez, E. Brillas, N. Oturan, M.A. Oturan, Catalytic
600 behavior of the $\text{Fe}^{3+}/\text{Fe}^{2+}$ system in the electro-Fenton degradation of the antimicrobial
601 chlorophene, Appl. Catal. B Environ. 72 (2007) 382–394.
- 602 [49] M.E.H. Bergmann, J. Rollin, T. Iourtchouk, The occurrence of perchlorate during
603 drinking water electrolysis using BDD anodes, Electrochim. Acta. 54 (2009) 2102–
604 2107.
- 605 [50] A. Vacca, M. Mascia, S. Palmas, A. Da Pozzo, Electrochemical treatment of water
606 containing chlorides under non-ideal flow conditions with BDD anodes, J. Appl.
607 Electrochem. 41 (2011) 1087–1097.
- 608 [51] C. Salazar, I. Sires, R. Salazar, H. Mansilla, C. Zaror, Treatment of cellulose bleaching
609 effluents and their filtration permeates by anodic oxidation with H_2O_2 production, J.
610 Chem. Technol. Biotechnol. 90 (2015) 2017–2026.
- 611 [52] E. Lacasa, J. Llanos, P. Cañizares, M.A. Rodrigo, Electrochemical denitrification with
612 chlorides using DSA and BDD anodes, Chem. Eng. J. 184 (2012) 66–71.
- 613 [53] J. Davis, J.C. Baygents, J. Farrell, Understanding Persulfate Production at Boron
614 Doped Diamond Film Anodes, Electrochim. Acta. 150 (2014) 68–74.
- 615 [54] K. Serrano, P.A. Michaud, C. Comninellis, A. Savall, Electrochemical preparation of
616 peroxodisulfuric acid using boron doped diamond thin film electrodes, Electrochim.
617 Acta. 48 (2002) 431–436.
- 618 [55] G.P. Anipsitakis, M.A. Gonzalez, Cobalt-Mediated Activation of Peroxymonosulfate

- 619 and Sulfate Radical Attack on Phenolic Compounds . Implications of Chloride Ions,
620 Environ. Sci. Technol. 40 (2006) 1000–1007.
- 621 [56] G. Merényi, J. Lind, S. Naumov, C. von Sonntag, Reaction of ozone with hydrogen
622 peroxide (peroxone process): a revision of current mechanistic concepts based on
623 thermokinetic and quantum-chemical considerations., Environ. Sci. Technol. 44 (2010)
624 3505–3507.
- 625 [57] C.A. Martínez-Huitle, E. Brillas, Electrochemical alternatives for drinking water
626 disinfection., Angew. Chem. Int. Ed. Engl. 47 (2008) 1998–2005.
- 627 [58] Y. Honda, T.A. Ivandini, T. Watanabe, K. Murata, Y. Einaga, An electrolyte-free
628 system for ozone generation using heavily boron-doped diamond electrodes, Diam.
629 Relat. Mater. 40 (2013) 7–11.
- 630 [59] P. Christensen, T. Yonar, K. Zakaria, The Electrochemical Generation of Ozone : A
631 Review, Ozone Sci. Eng. 35 (2013) 149–167.
- 632 [60] A. Kapałka, G. Fóti, C. Comninellis, Kinetic modelling of the electrochemical
633 mineralization of organic pollutants for wastewater treatment, J. Appl. Electrochem. 38
634 (2008) 7–16.
- 635 [61] N. Oturan, E.D. Van Hullebusch, H. Zhang, L. Mazeas, H. Budzinski, K. Le Menach,
636 M.A. Oturan, Occurrence and removal of organic micropollutants in landfill leachates
637 treated by electrochemical advanced oxidation processes, Environ. Sci. Technol. 49
638 (2015) 12187–12196.
- 639 [62] K. Brudnik, D. Wójcik-pastuszka, J.T. Jodkowski, J. Leszczynski, Theoretical study of
640 the kinetics and mechanism of the decomposition of trifluoromethanol,
641 trichloromethanol, and tribromomethanol in the gas phase, J. Mol. Model. 14 (2008)
642 1159–1172.
- 643 [63] R. Mertens, C. von Sonntag, J. Lind, G. Merenyi, A Kinetic Study of the Hydrolysis of

644 Phosgene in Aqueous Solution by Pulse Radiolysis, *Angew. Chemie Int. Ed. English*.
645 33 (1994) 1259–1261.
646 [64] C. Von Sonntag, *Advanced oxidation processes: Mechanistic aspects*, *Water Sci.*
647 *Technol.* 58 (2008) 1015–1021.
648
649

FIGURE CAPTIONS

650
651

652 **Fig. 1.** Reactor set-up for H₂O₂ oxidation and electrolysis experiments.

653
654 **Fig. 2.** Evaluation of CCl₄ electroactivity and reactivity with H₂O₂. (A), cyclic
655 voltammogrammes in absence or presence of CCl₄ with Pt working electrode (Pt counter
656 electrode); (B), cyclic voltammogrammes in absence or presence of CCl₄ with glassy carbon
657 working electrode (Pt counter electrode), (C), oxidative treatment of CCl₄ with hydrogen
658 peroxide.

659

660 **Fig. 3.** Hydrogen peroxide concentration evolution during spiking experiment.

661

662 **Fig. 4.** Degradation of CCl₄ by AO and EF treatments using different cathodes and anodes.

663 (A), chloride concentration ([Cl⁻]) evolution normalized by the maximal theoretical Cl⁻
664 concentration ([Cl⁻]_{max,th}) and (B), determination of the apparent rate constants for CCl₄ decay
665 assuming a pseudo-first order kinetic model (SI, Eq. 15). EF, electro-Fenton; AO, anodic
666 oxidation; CF, carbon felt; SS, stainless steel; BDD, boron-doped diamond.

667

668 **Fig. 5.** Hydrogen peroxide accumulation using SS cathode and Pt anode. Conditions: $I = 1000$
669 mA, [Na₂SO₄] = 50 mM, $V = 200$ mL, pH 3.

670

671 **Fig. 6.** Chromatograms of anions evolution during EF treatments of CCl₄ with BDD anode
672 (EF-CF-BDD) at different treatment time (0 min, 20 min, 40 min, 60 min, 120 min, 240 min).
673 (A), ionic chromatograms. (B), Cl⁻ peaks evolution. (C), SO₄²⁻ peaks evolution. Conditions: I
674 = 1000 mA, [Na₂SO₄] = 50 mM, [Fe²⁺] = 0.05 mM, $V = 200$ mL, pH 3.

675

676 **Fig. 7.** Hydrogen peroxide accumulation using CF cathode and Pt anode. Conditions: $I = 1000$
677 mA, [Na₂SO₄] = 50 mM, $V = 200$ mL, pH 3.

678

679 **Fig. 8.** Chromatograms of anions evolution during electro-Fenton treatments of CCl₄ with Pt
680 anode (EF-CF/Pt) at different treatment time (0 min, 5 min, 10 min, 20 min, 40 min, 60 min,
681 120 min, 180 min, 240 min). (A), ionic chromatograms. (B), Cl⁻ peaks evolution. (C), SO₄²⁻
682 peaks evolution. Conditions: $I = 1000$ mA, $[\text{Na}_2\text{SO}_4] = 50$ mM, $[\text{Fe}^{2+}] = 0.05$ mM, $V = 200$
683 mL, pH 3.

684
685 **Fig. 9.** Mineralization of CCl₄ by anodic oxidation and electro-Fenton treatments using
686 different cathodes and anodes. (A), normalized TOC evolution by the initial TOC. (B),
687 determination of the TOC decay rate constants assuming a pseudo-first order kinetic model.
688 EF, electro-Fenton; AO, anodic oxidation; CF, carbon felt; SS, stainless steel; BDD, boron-
689 doped diamond.

690
691 **Fig. 10.** Pathways of organic compounds oxidation by [•]OH. (A), CCl₄ oxidation by ipso-
692 substitution with [•]OH. (B), schematic description of the four attack modes of [•]OH with
693 organic compounds. RH, alkane; ArH, aromatic; C_xX_y, perhalogenocarbon compounds.

694

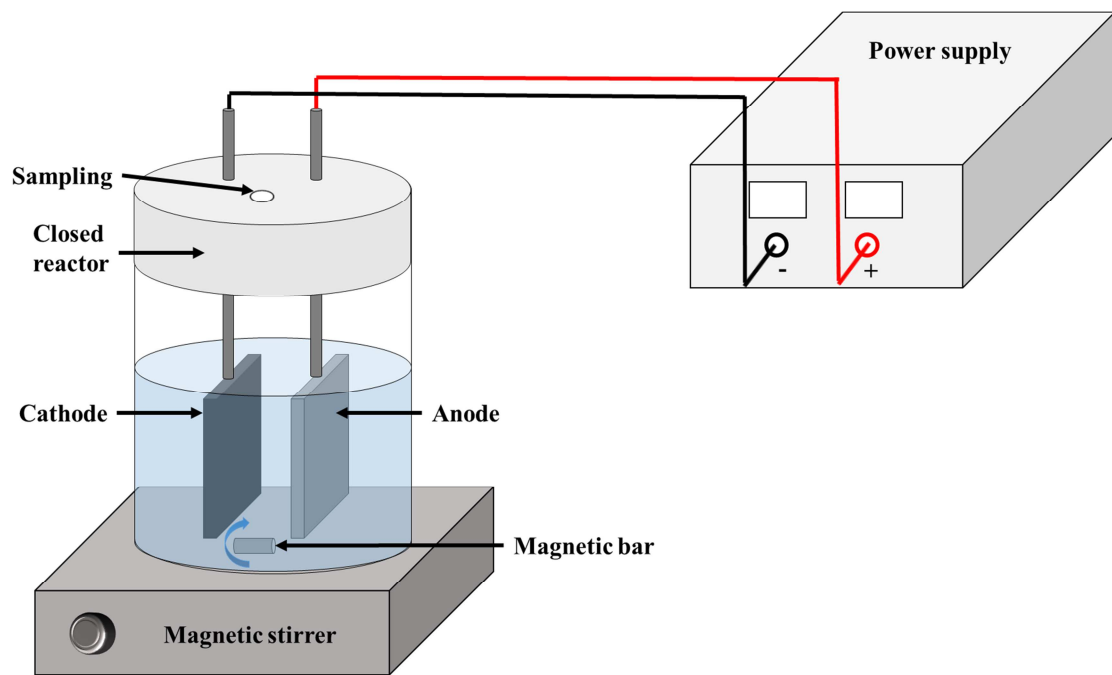


Fig. 1

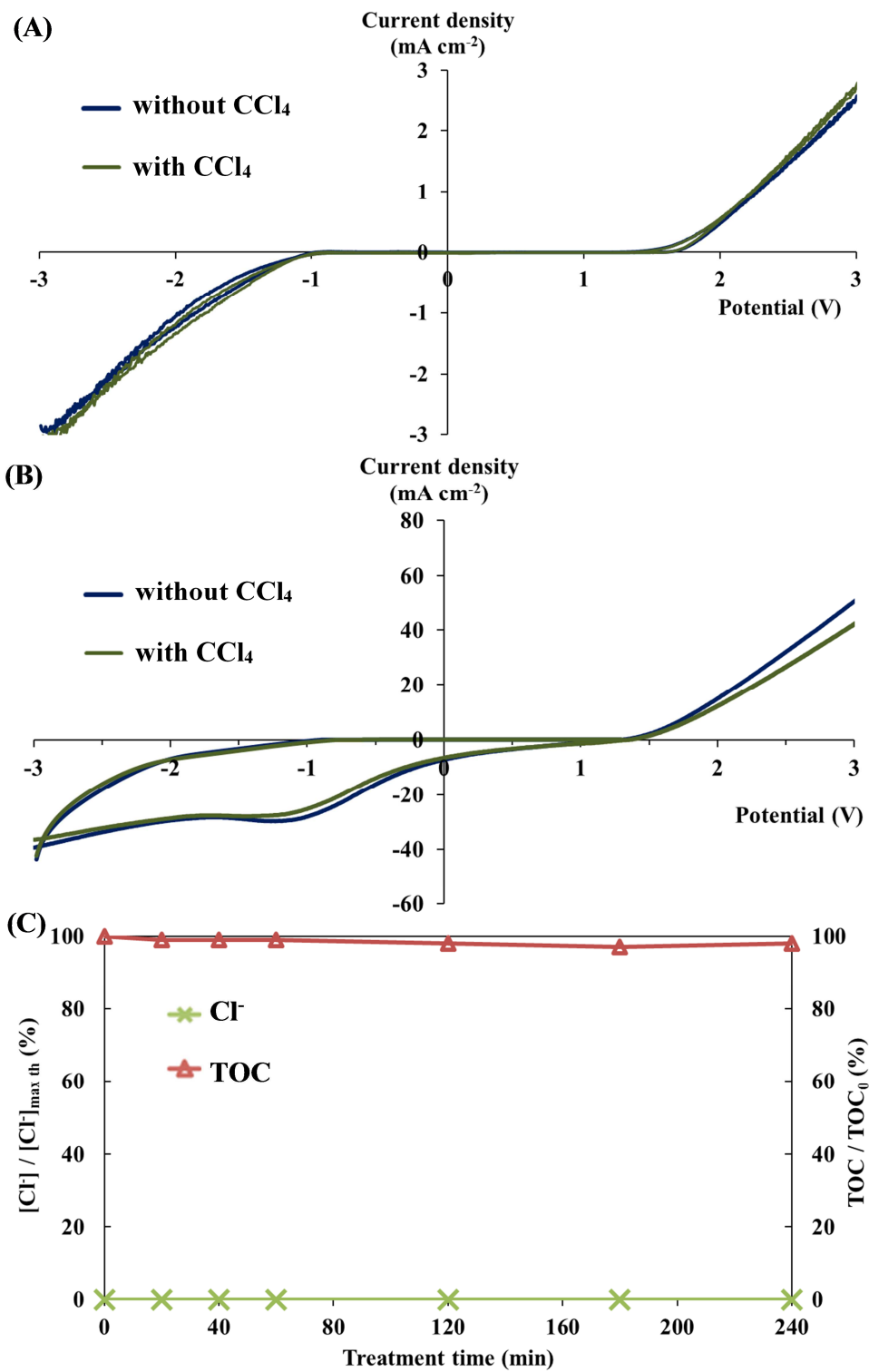


Fig. 2

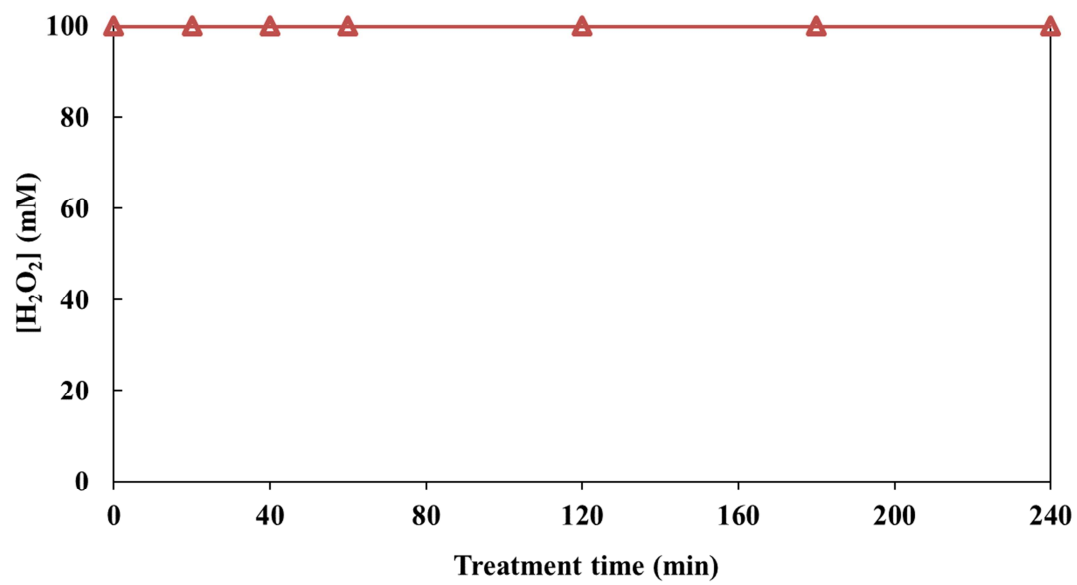


Fig. 3

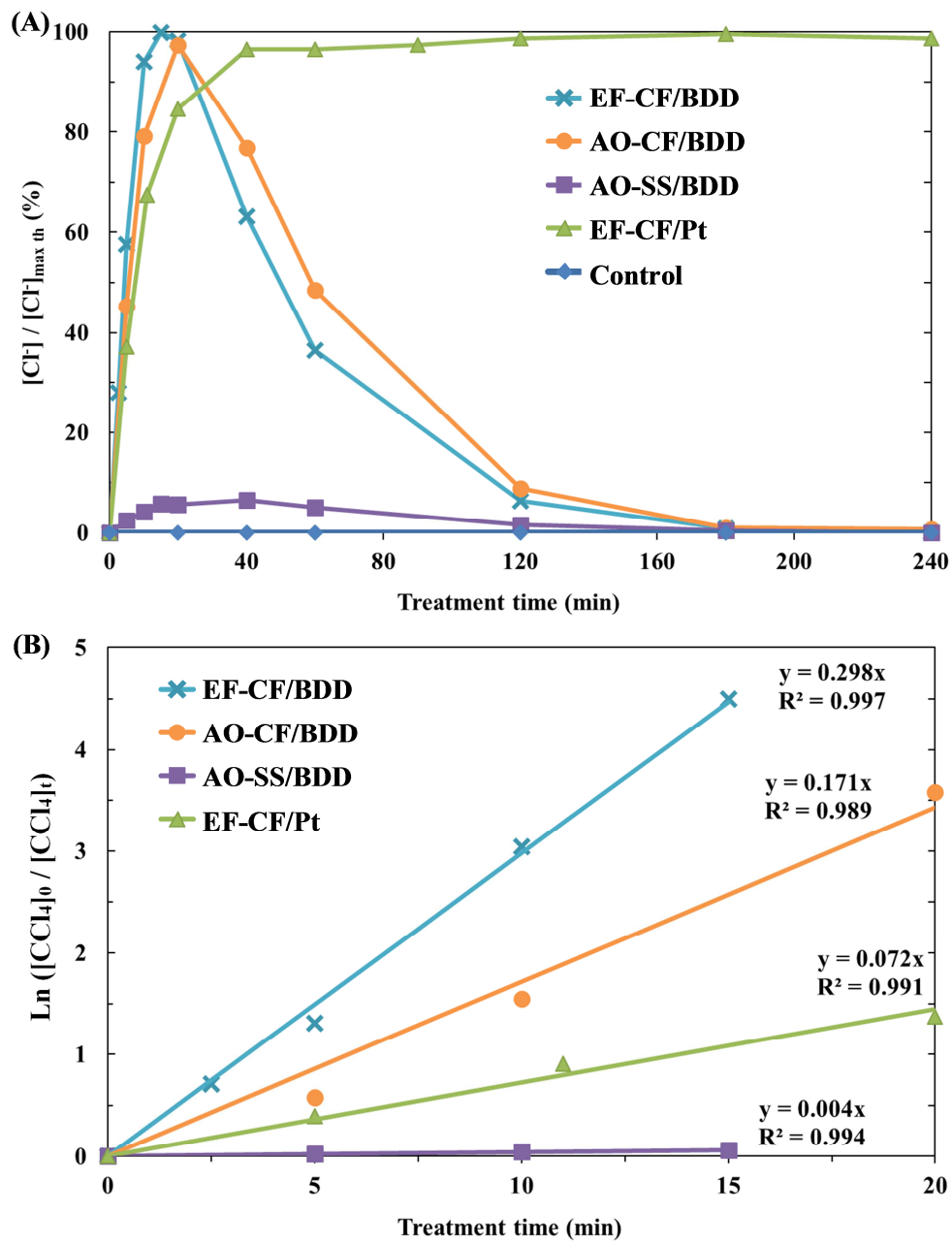


Fig. 4

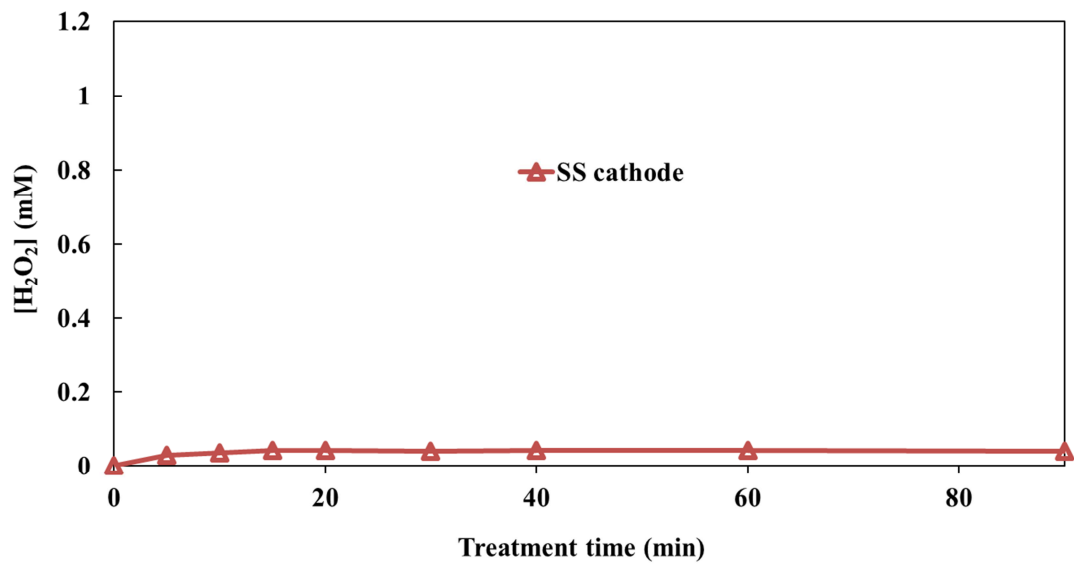


Fig. 5

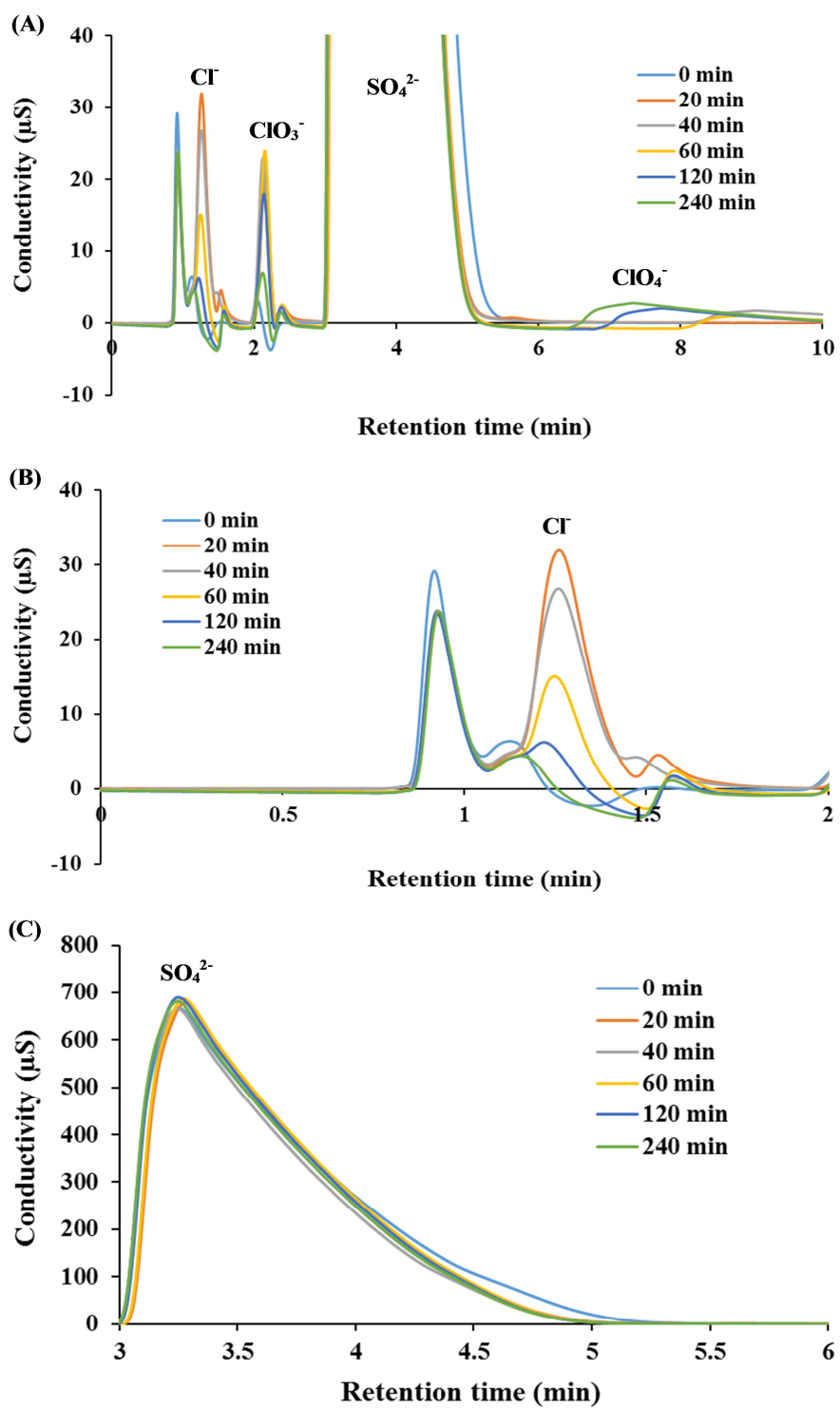


Fig. 6

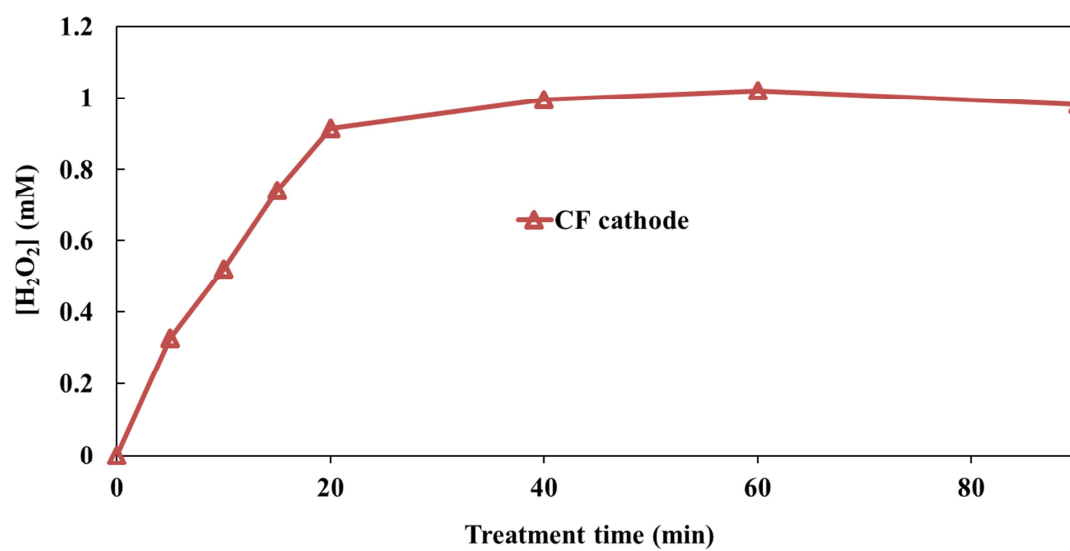


Fig. 7

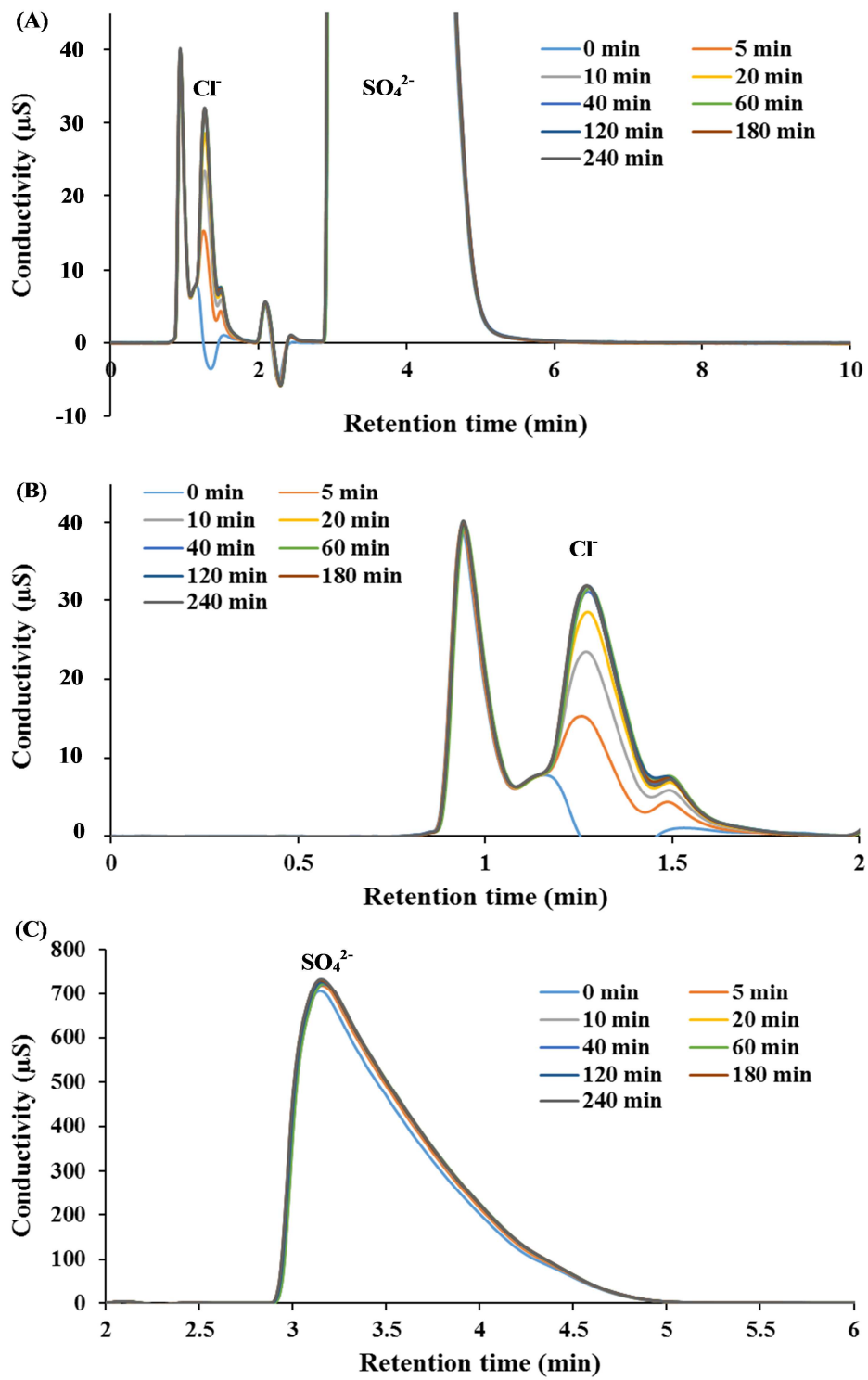


Fig. 8

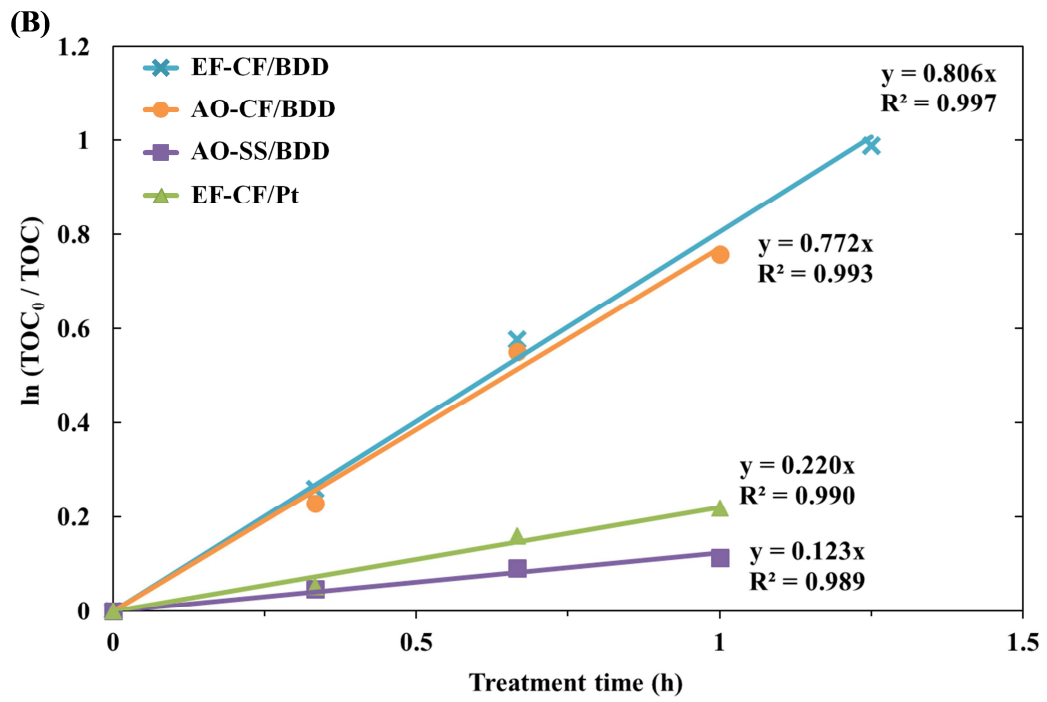
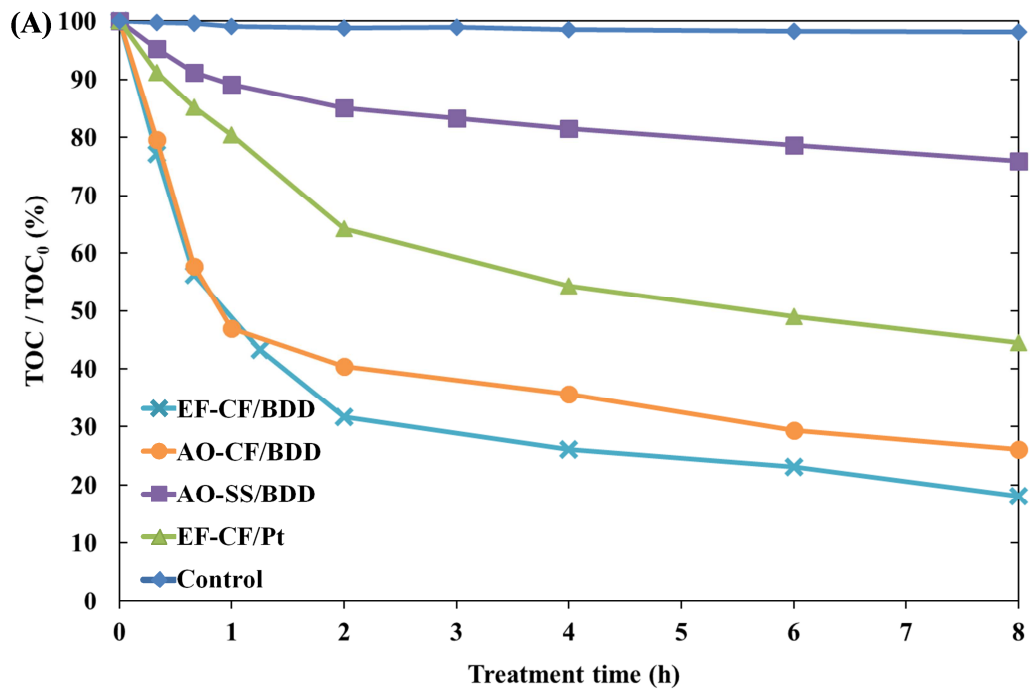


Fig. 9

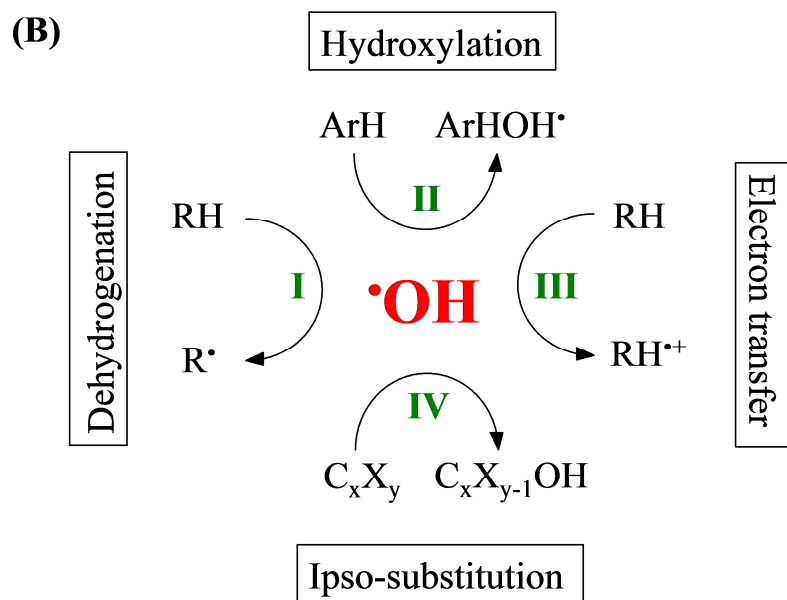
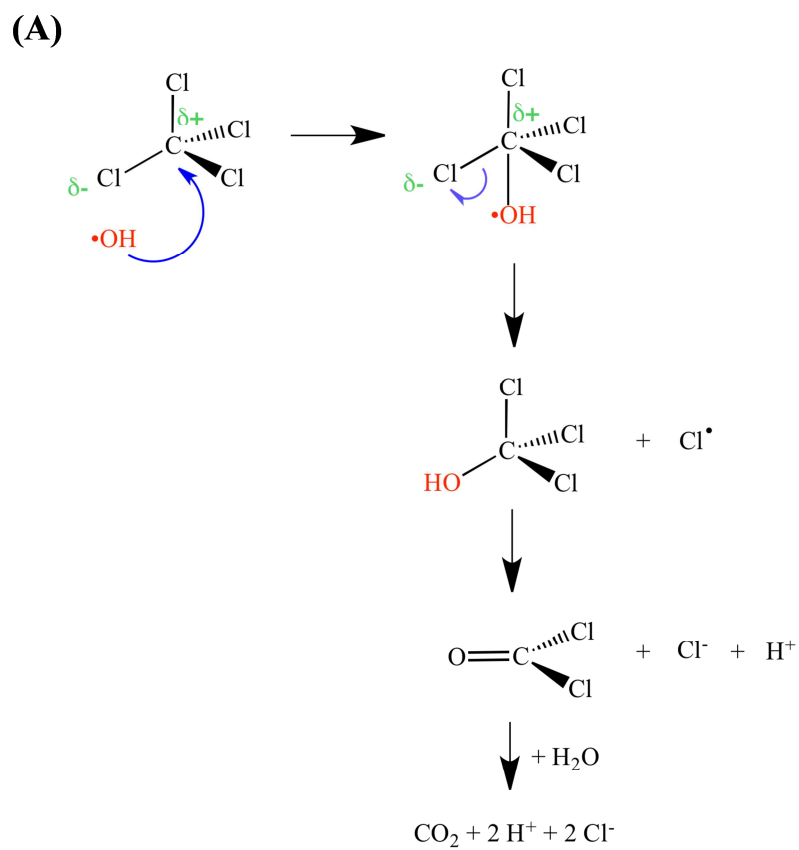


Fig. 10